Nucleic Acid Hybridization Enhanced Luminescence for Rapid and Sensitive RNA and DNA Based Diagnostics

Cui Liu, Xiaoyuan Wei, Huimin Zhang, Mingzhen Zhang, Xue-Feng Yu, Niko Hildebrandt, Qing-Ying Luo, Zongwen Jin

Nucleic Acid Hybridization Enhanced Luminescence for Rapid and Sensitive RNA and DNA Based Diagnostics

Cui Liu,[#] Xiaoyuan Wei,[#] Huimin Zhang, Mingzhen Zhang, Xue-Feng Yu, Niko Hildebrandt, Qing-Ying Luo,[*] Zongwen Jin[*]

ABSTRACT: Long-lived emissive nucleic acid probes are widely used in biochemical analysis due to their programmable structures, high signal-to-background ratio, and high sensitivity. Homogeneous detection based on long-lived emissive nucleic acid probes is often achieved through Förster resonance energy transfer (FRET), which suffers from the limitation of a narrow effective distance range. Herein, a new strategy of accessing nucleic acid hybridization-responsive luminescent probes is presented. The photoluminescence (PL) of a Lumi4-Tb complex internally modified with DNA is switched on by nucleic acid hybridization, after which the PL is increased up to 20 times. PL lifetime analysis revealed a possible mechanism of luminescence enhancement. Due to the flexibility of single-stranded nucleic acid chains, the bases and phosphate groups can coordinate with the Tb (III), which reduces the stability of the Tb complex and results in weak PL. After hybridization, the rigid double helix structure suppresses the coordination between Tb(III) and the bases or phosphate groups, causing luminescence enhancement. As the DNA sequence can be freely designed, an array of probes for different DNA or RNA targets can be created with the same Tb complex. Moreover, the novel probe design can afford pM detection limits of DNA or RNA without any nucleic acid amplification and exhibits a great potential for nucleic acid detection in clinical diagnosis.

Nucleic acid probes are widely used in the detection of biological analytes, such as enzymes, proteins, small biological molecules, metal ions, nucleic acids, and even cells, due to their variable structure, simple synthesis, and easy modification.[1-3] Nucleic acid signal amplification provides an important platform for the detection of low-abundance substances, improves the sensitivity of nucleic acid probes, and is essential for biomedical research, molecular diagnosis, and pharmacogenomics.[4-6] Among the many nucleic acid probes, fluorescent ones play a crucial role in analytical chemistry due to their high sensitivity, diversified designs, and desired quantitative analysis capability.[7] Generally, fluorescent nucleic acid probes are designed based on the combination between probe and target, which can induce structural changes of the nucleic acid and then initiate the fluorescence signal switch. Common fluorophores for nucleic acid labeling include organic dyes, metal (e.g., silver and copper) nanoclusters, and lanthanides. Compared to organic dyes and nanomaterials with nanosecond-lifetime luminescence, the PL lifetime of lanthanides can reach milliseconds.[8-10] Moreover, time-resolved or time-gated detection can be used to eliminate the interference of background luminescence and light scattering, improving the signal-to-background ratio and finally realizing high-sensitive detection in complicated biological environments containing many endogenous fluorophores.[11-14] For example, single-stranded oligonucleotides could enhance the emission of Eu^{3+} and Tb^{3+} ions in solution, which has been employed to detect ions, small molecules,[15, 16] distorted DNA regions,[17] and DNA- and RNA-drug interactions.[18] The energy transfer from nucleic acids to Tb(III) was also used to detect single DNA mismatches.[19] However, assays based on nucleic acid or nucleotide-enhanced luminescence of rare-earth ions suffer from poor anti-interference capability caused by the interaction between lanthanide ions and small molecules, nucleic acids, or proteins in biological systems. To overcome this problem, a variety of macrobicyclic ligands have been used in preparing luminescent lanthanide complexes.[20-26] The octadentate cages of Tb(III) 2-hydroxyisophthalamides exhibit exceptionally high quantum yields ($\Phi_{total} \geq 50\%$), large extinction coefficients ($\varepsilon_{max} \geq 20{,}000\ M^{-1}cm^{-1}$), and long lifetimes ($\tau \geq 2.45$ ms).[24] More importantly, the octadentate macrotricyclic terbium (III) can retain these properties for a long term, even after bioconjugation to proteins such as streptavidin, bovine gamma globulin, bovine serum albumin, and mouse IgG. In our previous works, the Tb(III) complex was employed as the donor to develop a series of FRET sensing systems for the homogeneous detection of nucleic acids.[27-29] Hybridization gave rise to a close distance between Tb(III) and different acceptors, such as dyes or quantum dots, which caused FRET-sensitized long-lived acceptor PL for time-gated detection. Multiple nucleic acids could be quantitatively detected simultaneously by employing FRET acceptors with separated PL emission peaks. Unfortunately, FRET can only occur within a narrow distance range (2-10 nm). In actual detections, especially when nanomaterials or biological macromolecules are involved, the distance between the donor and acceptor might be out of the FRET distance range, resulting in low sensitivity that does not meet application requirements.

Here, we propose a novel method to enhance the PL of lanthanide complexes via nucleic acid hybridization. Based on the new principle, a simple, rapid and sensitive universal assay could be designed for point of care testing (POCT). The terbium complex (Lumi4-Tb) conjugated to the single-stranded nucleic acid at an internal position exhibits low luminescence intensity. After hybridization with the complementary chain, the PL of Lumi4-Tb increased up to 20 times. Through PL lifetime analysis, the principle of nucleic acid hybridization-enhanced emission was proposed. Due to the flexibility of single-stranded nucleic acids, the bases or phosphate groups can coordinate with the Tb(III), which reduces the stability of Lumi4-Tb and results in low luminescence intensity. After hybridization, the formation of a rigid double helix structure inhibits the coordination between the bases/phosphate and Tb(III), leading to luminescence enhancement. Based on this principle, rapid detection of nucleic acid targets with an ultralow detection limit of 17 pM was achieved without any DNA amplification. With the introduction of DNA ligase, high-sensitivity and high-specificity detection of miR-20a was accomplished with a detection limit of 23 pM. It was also used in the detection of the cDNA of the COVID-19 virus (part of genome sequence), with a detection limit of 27 pM.

Moreover, this new method could be used to detect miRNA-21 levels in real biological samples of breast cancer patients and healthy persons. The nucleic acid hybridization-enhanced luminescence detection method possesses the advantages of high universality, rapidity, and simplicity and can be used potentially in the highly sensitive detection of various nucleic acids, proteins, and other small biological molecules under physiological conditions.

EXPERIMENTAL SECTION

Preparation of Tb-DNA conjugates

Briefly, amino modified oligonucleotides were mixed with 8 times molar excess amount of Lumi4-Tb-NHS in 25 mM HEPES buffer (pH 7.4) containing EDC with a concentration of 1 mg/mL. The mixtures were incubated overnight at room temperature. The Tb-DNA conjugates were separated from Lumi4-Tb and other impurities by using PD-10 Desalting Columns (GE Healthcare), which was pre-equilibrated with a HEPES buffer (25 mM, pH 7.4). The concentrations of all elution fractions were analyzed by monitoring the absorbance at 260 nm (Denovix, DS-11 spectrophotometer/Fluorometer series). The concentrations of all fractions were adjusted to be 5 nM, and then their fluorescence intensities were measured in the time window of 100-600 μs. The early fractions that exhibited the same fluorescence intensities were pooled and stored for use.

DNA and RNA assays

All the assays were performed on a Victor X4 fluorescence plate reader (PerkinElmer) by measuring time-gated intensity. Total sample volumes in the microwells were always 100 μL. For DNA and RNA assays, 25 mM HEPES buffer containing 150 mM NaCl was used as the reaction solution. The probe with a concentration of 5 nM was mixed with the corresponding target with a series of concentrations. All samples were prepared three times and measured once on a plate reader (Victor X4) with time-gated (100-600 μs) fluorescence intensity detection using a bandpass filter with 494±10 nm.

MiR-20a assays

A series doses of miR-20a were added to the P11 with a final concentration of 10 nM, P10-Tb with a final concentration of 2 nM, and an appropriate amount of target miRNA was prepared in the optimized SplintR DNA ligase reaction buffer (pH 7.6, 50 mM Tris-HCl, 10 mM $MgCl_2$, 1 mM ATP 10 mM DTT). Then, SplintR DNA ligase (20U) was added to the mixture. The reaction solution of 100 μL was incubated in black 96-well microtiter plates at 37 °C for 30 min and then measured on a plate reader (Victor X4) with time-gated (100-600 μs) fluorescence intensity detection using bandpass filter with 494±10 nm.

Detection of MiR-21 in clinical samples

Total RNA extraction from peripheral blood samples was performed according to the protocol of miRNeasy Mini Kit (Qiagen, product No.1038703). For miRNA21 detecting, 10 ug/mL RNA sample was added into 100μL reaction solution (25 mM HEPES and 150 mM NaCl, pH 7.4), which contain P16-Tb with a final concentration of 3 nM. The reaction solution of 100 μL were incubated in black 96-well microtiter plates at room temperature for 4 h and then measured on a plate reader (Victor X4) with time-gated (100-600 μs) fluorescence intensity detection using bandpass filter with 494±10 nm.

RESULTS AND DISCUSSION

Tb(III) is one of the most used lanthanide ions due to its high intrinsic quantum yield and visible emission. Herein, the terbium complex Lumi4-Tb (Tb) functionalized with sulfo-N-hydroxysuccinimide (NHS) ester[26] was conjugated to amino-modified DNA to obtain luminescent probes. The Lumi4-Tb exhibited four characteristic sharp emission peaks at 488, 545, 586, and 620 nm (**Figure S1**), which could be assigned to the $5D4 \rightarrow 7FJ$ luminescence transitions.[26]

We designed a series of DNAs with 32 nucleotides (P1-5) to conjugate with Lumi4-Tb through modified amino groups at different positions (**Table S1**). The Lumi4-Tb labeled DNAs were separated from the excess Lumi4-Tb and other impurities by using desalting columns. As shown in **Figure 1A**, the emission spectra of the DNA-Tb conjugates were almost identical to Lumi4-Tb. However, P2-Tb, P3-Tb, P4-Tb, and P5-Tb, in which Tb was bound to internal modified amino groups, exhibited much lower PL intensities than the P1-Tb bound with Lumi4-Tb through the amino group modified at 5'-end, suggesting that internal modification could decrease the luminescence of Lumi4-Tb. After hybridization with the complementary target DNA, the PL intensities of P2-Tb, P3-Tb, P4-Tb, and P5-Tb increased up to 2.5 to 4.0 times. In contrast, that of P1-Tb showed a relatively stable luminescence (**Figure 1B-C** and **Figure S2**), indicating the internally modified Lumi4-Tb of DNA was more sensitive to the structural changes induced by hybridization.

To reveal the mechanism of the enhanced luminescence of Lumi4-Tb labelled DNAs, time-resolved PL decay profiles of these probes before and after hybridization with the complementary chains were measured at the maximum emission peak at 545 nm by using 340 nm as the excitation

wavelength. Lumi4-Tb exhibited a linear plot of the log intensity versus time, indicating its single exponential decay with a lifetime of 2.77 ms (**Figure 1D**). The P1-Tb before and after hybridization with the complementary chain also exhibited single-exponential decay curves (**Figure 1E**) with a similar lifetime of 2.64 ms, suggesting the emission property of the Lumi4-Tb was retained upon conjugation to the end of DNAs.

When Lumi4-Tb was conjugated to DNAs at an internal position, the time-resolved decays required a triple exponential decay function of the form $I_{(t)} = y_0 + A_1 exp^{(-t/\tau_1)} + A_2 exp^{(-t/\tau_2)} + A_3 exp^{(-t/\tau_3)}$ to fit (**Figure 1D**), producing components with one long lifetime of circa 2.2 ms to 2.8 ms (τ_1) and two short lifetimes of circa 80 μs to 120 μs (τ_2) and circa

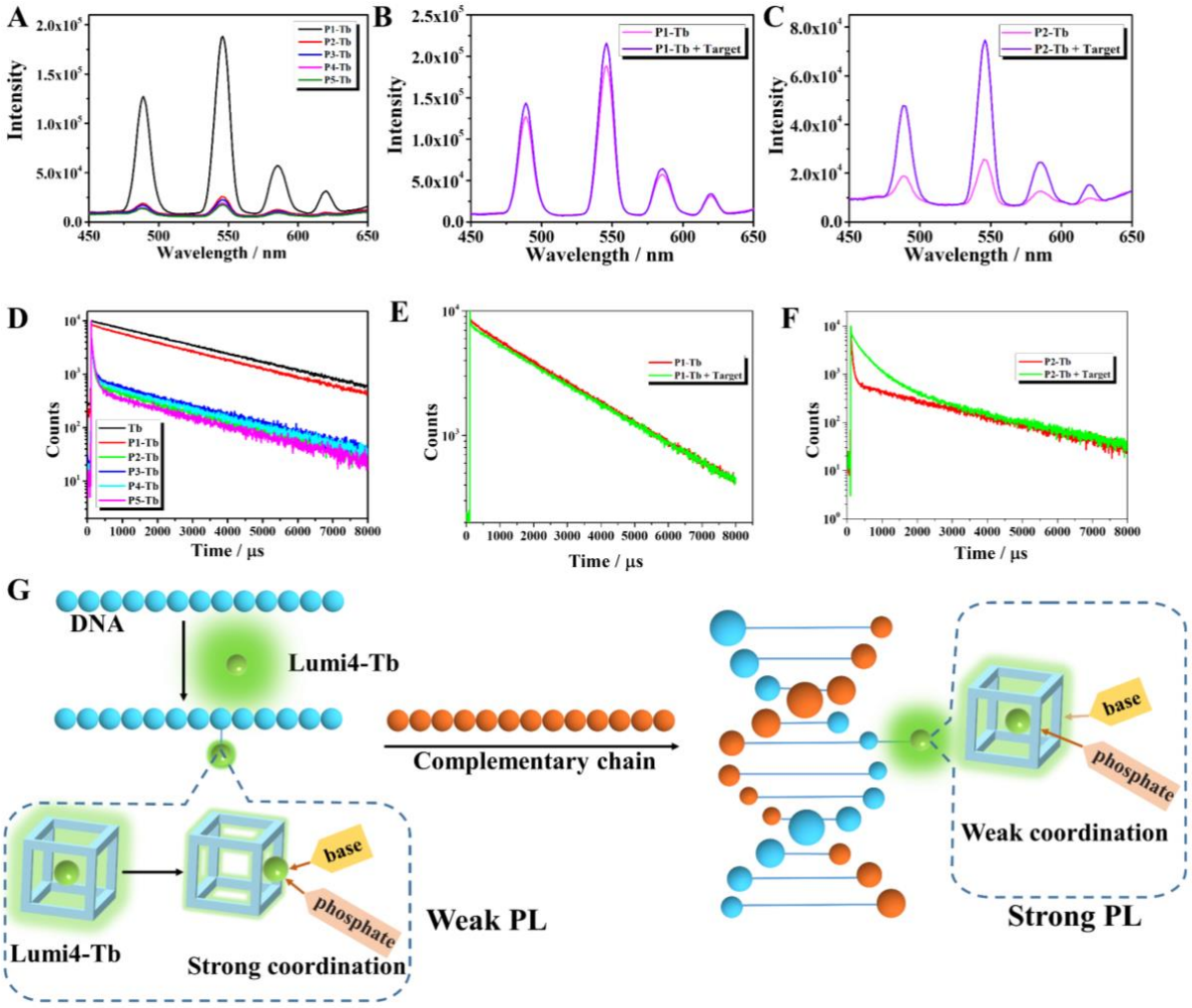

Figure 1. (A) Luminescence spectra of Lumi4-Tb labeled probes with the same concentration of 100 nM, comparison of luminescence spectra of P1-Tb (B) and P2-Tb (C) before and after hybridization with the target, PL decays of Tb before and after conjugated with DNAs at different positions (D), comparison of PL decay curves of P1-Tb (E) and P2-Tb (F) before and after hybridization with the complementary strands, and schematic presentation of the proposed mechanism of nucleic acid hybridization-enhanced luminescence, for which single-stranded DNA destabilizes the Tb complex through base/phosphate interaction and double-stranded DNA stabilizes the Tb complex (G).

30 μs (τ_3). The resulting fit parameters were summarized in **Table 1**. We attributed the long component to quenched PL caused by the interaction of DNA with the Lumi4-Tb complex and the two short components to quenched PL caused by coordination between the Tb(III) ion and the structure of DNA. Previous work has shown the binding of nucleic acids and Tb(III) and found that both phosphate groups and bases could bind to Tb(III).[17] Pyrimidine nucleotides (CMP and TMP) were mainly combined with rare-earth ions through phosphate groups, and the contribution of bases was small, whereas the phosphate groups and bases of purine nucleotides (AMP and GMP) were both involved in coordination. In addition, there might also be a synergistic effect between the phosphate groups and the bases. Therefore, we speculated that the short lifetime components were related to the coordination of the phosphoric acid groups and the bases with the Tb central ion. After hybridization, the decay of PL intensities of P(2-5)-Tb with time became significantly slower (**Figure 1F**, **Figure S4**). The resulting fit parameters showed that the long component ($A_1 exp^{(-t/\tau_1)}$) decreased slightly in lifetime and significantly in

amplitude fraction, the first short components ($A_2 exp^{(-t/\tau_2)}$) did not change significantly, and the second short component ($A_3 exp^{(-t/\tau_3)}$) disappeared. In addition, a new medium lifetime component (~0.45 to 0.65 ms) appeared with a strong amplitude fraction (circa 40 to 50%). These significant changes in the overall PL quenching must be related to the formation of double-stranded DNA. A possible explanation was the coordination of the nitrogen within the bases to the Tb(III) ions in an open ssDNA form (resulting in competition with the Lumi4 complex and thus increased PL quenching), which would be suppressed in the case of the double-helical structure of dsDNA. This agrees with the finding that single-stranded oligonucleotides can enhance the PL of Tb(III) (due to coordination), but purified duplexes do not.[17] However, in our case, instead of enhancement (from pure Tb(III) to DNA-coordinated Tb(III)), we saw a quenching (from Lumi4-coordinated Tb(III) to DNA-coordinated Tb(III)). We hypothesized that the coordination between the base and Tb(III) was entirely suppressed in the dsDNA structure (disappearance of the shortest lifetime). In contrast, the phosphoric acid group located at the edge of the double helix structure continued to compete with the original ligand of Lumi4-Tb but with an overall weaker contribution (translated as a new medium lifetime component).

To further confirm that the PL quenching was caused by interaction with the Tb(III) ions and not by structural changes in the Lumi4 complex, we performed UV-Vis absorption experiments. The UV-Vis spectra of ssDNA, Tb-ssDNA, and the mix of Tb-ssDNA and the complementary strand showed no obvious differences in both the DNA absorption around 260 nm and the Lumi4 absorption around 350 nm (**Figure S3**), suggesting that no significant structural change occurs during the interaction between DNA and the Lumi4 complex. Although our PL and UV-Vis investigations and the previous studies[15, 16, 19] led to reasonable assumptions concerning the mechanism of interaction, a more profound study (including, e.g., FT-IR and Raman spectroscopy) would be necessary to further elucidate the exact Lumi4-Tb-nucleic acid interaction. However, concerning the biosensing principle, the actual result of the interaction (change of PL lifetime) is more important than the exact mechanism. Thus, we did not investigate the mechanism in further detail but instead focused on the bioanalytical application.

Table 1. Summary of the PL lifetime of Tb and P-Tb before and after hybridization.

	τ_1 (µs)	rel. A_1 [a]	τ dsDNA (µs)	rel. A [a]	τ_2 (µs)	rel. A_2 [a]	τ_3 (µs)	rel. A_3 [a]	χ^2 [b]
Lumi4-Tb	2768 ± 6	100%							1.046
P1-Tb	2638 ± 12	99.0%			362 ± 40	1.0%			1.148
P1-Tb+Target	2696 ± 11	99.4%			242 ± 30	0.60%			1.118
P2-Tb	2360 ± 22	84.8%			79 ± 7	7.5%	28 ± 2	7.8%	1.156
P2-Tb+Target	2214 ± 49	42.8%	447 ± 7	51.8 %	100 ± 6	5.5%			1.170
P3-Tb	2501 ± 23	88.6%			121 ± 9	5.1%	28 ± 1	6.3%	1.108
P3-Tb+Target	2272 ± 42	56.5%	494 ± 11	38.7 %	121 ± 8	4.8%			1.050
P4-Tb	2413 ± 22	87.0%			95 ± 8	6.6%	30 ± 2	6.4%	1.027
P4-Tb+Target	2187 ± 59	56.1%	644 ± 16	38.2 %	99 ± 3	5.7%			1.053
P5-Tb	2444 ± 27	77.3%			95 ± 4	16.4%	29 ± 2	6.2%	1.147
P5-Tb+Target	2202 ± 38	53.8%	452 ± 8	38.8 %	86 ± 3	7.4%			1.104

a: rel. A refers to the fraction of the lifetime amplitudes A_1, A_2, and A_3. b: Fit quality factor (values close to unity are high quality).

Although steady-state PL assays indicate the concentration of an analyte by PL intensity, the signal can hardly be distinguished from background if the concentration of the analyte is low. Time-gated (TG) PL might solve this problem efficiently. For a proof-of-principle demonstration, we collected the integrated PL signals of these probes in a time range of 0.1 to 0.6 ms after pulsed excitations. As shown in **Figure 2A**, target binding to P1-Tb PL did not significantly influence the TG PL intensity, which was in agreement with the steady-state PL results (**Figure 1B**). In contrast, P2-Tb, P3-Tb, P4-Tb and P5-Tb showed significantly enhanced PL signals of 17, 13, 8, and 3-fold, respectively. With the best P2-Tb probe, the target could be quantified with a detection limit of 17 pM (**Figure 2B**). Notably, the assay required only a single fluorophore and a single DNA probe, and TG PL could be rapidly measured immediately after mixing probe and target. This simple, rapid, amplification-free, and sensitive assay might have great potential in nucleic acid-sensing and related clinical

and biological applications. DNAs have the advantages of easy availability, sequence diversity, conformational tunability, biocompatibility, and specific recognition capability, and have been widely used in the synthesis of functional probes. Therefore, arrays for different DNAs or RNAs can be created based on the nucleic acid hybridization enhanced luminescence principle.

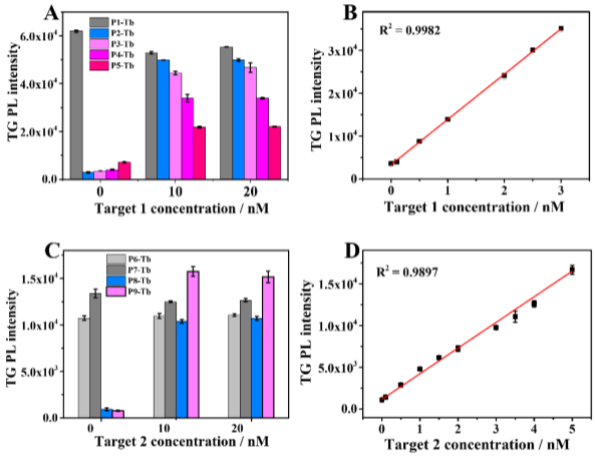

Figure 2. (A) TG PL intensity responses of different Tb-probes (5 nM) hybridizing to 32 nucleotides long target DNAs (target 1) at concentrations of 10 and 20 nM. (B) Assay calibration curve of TG PL intensity of P2-Tb as a function of target 1 concentration. (C) TG PL intensity responses of Tb-probes (5 nM) hybridizing to 17 nucleotides long target DNAs (target 2) at a concentration of 10 and 20 nM. (D) Assay calibration curve of TG PL intensity of P9-Tb as a function of target 2 concentration.

To verify the universality of the target detection principle, we designed a series of amino group-modified DNA probes with 17 nucleotides and conjugated them with Lumi4-Tb. As displayed in **Figure 2C**, the PL of the probes modified with Lumi4-Tb at the ends (3' and 5') did not increase in the presence of the complementary strand (target 2). However, when Lumi4-Tb was bound to the third or seventh base (T), target binding resulted in a ~20 and 12 fold PL enhancement, respectively. With the P9-Tb probe, target 2 could be sensitively quantified in the low and sub-nanomolar concentration range with a detection limit of 32 pM (**Figure 2D**).

We further attempted to expand our method to rapid and amplification-free assays for other RNA or DNA quantification. MicroRNA and a specific region of COVID-19-related DNA were employed as relevant model biomarkers due to their important and urgent clinical significance.

MicroRNAs (miRNAs) are a class of non-coding RNAs with 20-24 nucleotides. They act as post-transcriptional regulators in gene expression, thereby involving cell proliferation, migration, apoptosis, and canceration.[30] More than half of human genes are regulated by miRNAs, and one miRNA can have hundreds of target genes.[31-33] Many recent studies have demonstrated that the abnormal expression of miRNA was closely related to severe diseases such as cancer.[34] In addition, miRNA can exist in a very stable form in human peripheral blood circulation,[35] making them next-generation biomarkers for disease diagnosis and prognosis.[36, 37] Compared with previous nucleic acid targets, miRNAs are shorter, with a lower concentration and stronger homology. For example, there is only a 2-bases difference between miR-20a and miR-20b. Therefore, the accurate detection of miRNA is facing a huge clinical challenge. In order to achieve highly specific detection, we introduced the SplintR Ligase into miR-20a detection. SplintR ligase could efficiently catalyze the ligation of adjacent, single-stranded DNA splinted by a complementary RNA strand. Two DNA sequences (P10 and P11) those hybridize with the target miR-20a (**Figure 3A**) were designed. Probe P10 contained 13 nucleotides that could hybridize with parts of miR-20a. Probe P11 had a complementary sequence to miR-20a as well as a hairpin structure to increase the molecular weight of the probe, thereby improving the separation efficiency after conjugation with Lumi4-Tb. The melting temperatures of P10 and P11 to miR-20a were 44.6 °C and 29.3 °C (in buffer with 150 mM NaCl), respectively, demonstrating the instability of the hybridization between P11 and miR-20a. In combination with SplintR ligase, the 5'phosphate-modified P11-Tb could be efficiently ligated to P10 in the presence of miR-20a, producing highly stable duplexes with a melting temperature of 56.6 ºC. The double-stranded target-probe RNA/DNA complexes enhanced the Tb PL in a target concentration manner, such that rapid, sensitive, and specific detection of miR-20a with a detection limit of 23 pM could be achieved (**Figure 3B**). Although the background fluorescence intensity seem relatively high, it is relatively stable and could be subtracted from the total signals in detections. Since the sequence of miRNA-20b has two nucleotide mismatches for Pb11, the hybridization with P11-Tb is very unstable with T_m of only 20.8 ℃, and the nucleotide at the nick end is not paired. So, it is difficult for SplintR Ligase to catalyze the ligation of P10 and P11-Tb. Therefore, the PL intensity of the probe in the presence of miR-20b at a concentration of 10 nM was only 15% of that in the presence of miR-20a with concentration of 1nM, indicating the excellent specificity of the assay (**Figure 3C**). To further validate the specificity of our method, the detection of single-nucleotide mismatches by our sensor was investigated. We designed a series of "reduced miR-20b", miR-20b(1-4), in which we changed one or two mismatched nucleotides of 20b to one mismatch compared to 20a (**Table S1)**. The results showed that the selectivity became worse the further the single-nucleotide mismatch was positioned from the sticky end (Figure S5). Considering that the flexible design of our probes can move the sticky end closer to the mismatch, distinction of most single-nucleotide mismatches should be possible with our detection principle.

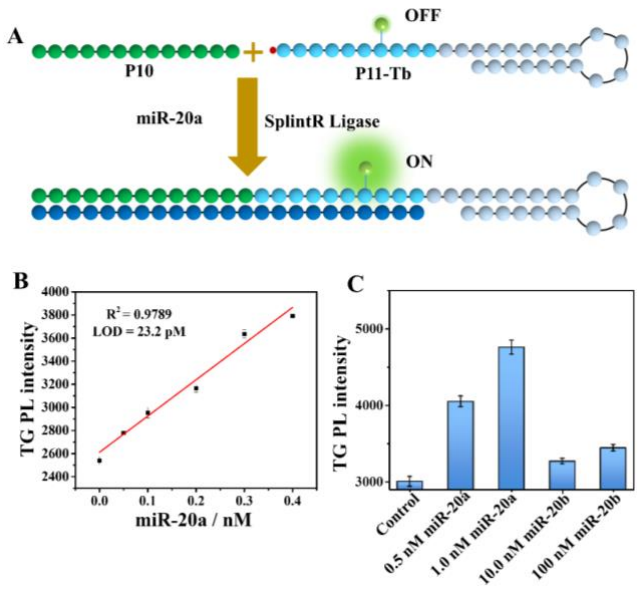

Figure 3. (A) Principle of miR-20a assay using SplintR ligase to ligate P11 and P10-Tb in the presence of miR-20a and producing a stable hybrid duplex, leading to PL enhancement of Tb. (B) Assay calibration curve of P11-Tb TG PL as a function of miR-20a concentration. (C) Assay specificity tested against miR-20b.

As witnessed worldwide for around two years, simple, rapid, and accurate detection of COVID-19 is essential for early diagnosis and disease management. Up to now, RT-PCR is still the preferred and most widely used method for the nucleic acid test of COVID-19 due to its simplicity, easy methodology, and extensively validated standard operating procedure. The viral RNA is converted into DNA by reverse transcription and DNA polymerization in RT-PCR. Bearing in mind for future application towards TG PL probe for RT-PCR, we replaced 6-carboxyfluorescein and blackberry quencher with Lumi4-Tb, while retaining the COVID-19 specific sequences of the WHO TaqMan probe,[38] to check if the PL enhancement indeed occurs using this probe sequence upon its complementary DNA (cDNA) hybridization. As the hairpin structure existed in the specific region of the ssDNA analogue of COVID-19 RNA (**Figure S6**) that reduced the hybridization with the complementary chain, we designed probe 12 (P12) with a hairpin structure at the 3'-end to recognize COVID-19 cDNA (**Figure 4A**). The cDNA target (**Figure 4B**) could be sensitively quantified at subnanomolar concentrations with detection limits of 27 pM.

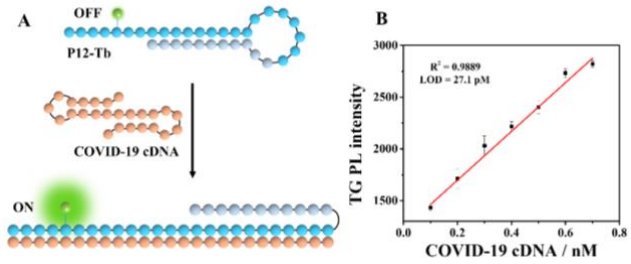

Figure 4. (A) Principle of COVID-19 hybridization assay. Linear relationship between TG PL and the concentration of COVID-19 cDNA (B).

In order to determine whether the new principle could be used in real biological samples, miR-21, a biomarker for breast cancer, in 16 peripheral blood samples (8 samples from breast cancer patients and 8 samples from healthy individuals) was selected as the target to detect. A series of probes with Lumi4-Tb modification at different positions were designed. As shown in **Figure 5A**, the Probe 16 (P16) with Lumi4-Tb modified at the 16th base (T) exhibited the optimal PL enhancement, which was employed in the assay of miR-21 (**Figure 5B**). The LODs of miRNA-21 reached 34 (**Figure 5C**) and 39 pM (**Figure S7**) in HEPES buffer and single stranded salmon sperm DNA solution (100 μg/mL), respectively, suggesting the high sensitivity of the assay. The values of R^2 for detection of miRNA was slightly lower than that for DNA detection, possibly due to miRNA is more easily degraded by RNases in the environment during storage and detection.

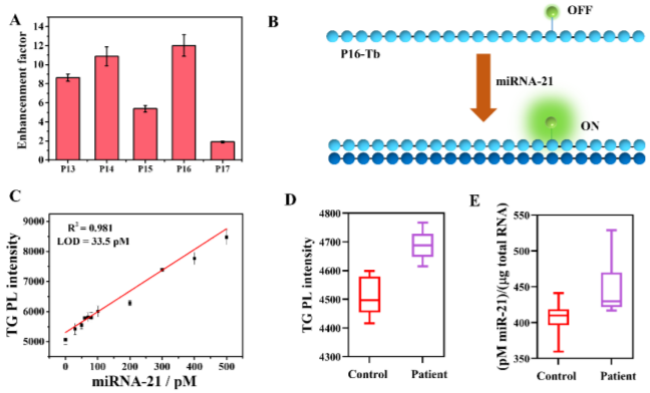

Figure 5. (A) TG PL enhancement factors of different Tb-probes (5 nM) hybridizing to cDNA at concentrations of 20 nM, (B) principle of miR-21 hybridization assay, linear relationship between TG PL and the concentration of miR-21 in HEPES (C), analysis of miR-21 in clinical samples by nucleic acid hybridization enhanced luminescence (D) and RT-qPCR (E).

To investigate whether the method works well complex biological matrix, we examined the PL enhancement of the P16-Tb in cell lysates. As shown in **Figure S8**, the TG PL intensities of P16-Tb in buffer and cell lysates with concentration of 50 and 500 μg/mL were same, indicating that the P16-Tb is stable in cell lysates. After added miR-21 (3nM), the intensity of P16-Tb cell lysates was stranger than that in buffer, may due to the presence of miR-21 in cell lysates. Moreover, P16 was used to detect miRNA-21 in the total miRNA extracted from the peripheral blood of breast cancer patients and healthy individuals, and the result indicated that the expression levels of miRNA-21 in the breast cancer patients was significantly higher compared to those in the healthy controls (**Figure 5D**). The result was consistent with that of qRT-PCR (**Figure 5E**), suggesting the great potential of the new principle for early cancer diagnosis.

In summary, nucleic acid hybridization-enhanced luminescence allowed facile, rapid, and sensitive TG PL assays for DNA and RNA quantification. The PL of Lumi4-Tb

modified internally in DNA could be enhanced significantly after hybridization. The coordination between Tb(III) and bases or phosphate groups was weakened by forming the rigid double helix structure. To exploit this principle, we designed a series of probes for different DNA and RNA targets and demonstrated sensitive, specific, washing-free, single-probe PL bioassays with picomolar detection limits without the use of any amplification steps. The performances of this new assay including LOD, specificity, linear range, and detection time are competitive even superior compared with other miRNA biosensors (Tabel S2). This versatile, simple, and rapid TG PL biosensor provides a strong potential for clinical diagnostics and point-of-care testing.

ASSOCIATED CONTENT

Supporting Information

The Suporting Information is available free of charge at http://pubsacs.org.
Additional experimental details, materials, methods, fluorescence spectra, fluorescence decay curves, and nucleic acid sequences used in this work.

AUTHOR INFORMATION

Corresponding Authors

Qing-Ying Luo – Materials Interfaces Center, Shenzhen Institutes of Advanced Technology, Chinese Academy of Sciences, Shenzhen 518055, P. R. China; orcid.org/0000-0002-0645-0278;
Email: qy.luo@siat.ac.cn
Zongwen Jin – Materials Interfaces Center, Shenzhen Institutes of Advanced Technology, Chinese Academy of Sciences, Shenzhen 518055, P. R. China;
Email: zw.jin@siat.ac.cn

Authors

Cui Liu – Department of Biophysics, School of Basic Medical Sciences, Xi'an Key Laboratory of Immune Related Diseases, Xi'an Jiaotong University Health Science Center, Xi'an, Shaanxi, 710049, P. R. China; orcid.org/0000-0002-8399-5765
Xiaoyuan Wei – Materials Interfaces Center, Shenzhen Institutes of Advanced Technology, Chinese Academy of Sciences, Shenzhen 518055, P. R. China
Mingzhen Zhang – Department of Biophysics, School of Basic Medical Sciences, Xi'an Key Laboratory of Immune Related Diseases, Xi'an Jiaotong University Health Science Center, Xi'an, Shaanxi, 710049, P. R. China.
Huimin Zhang – The First Affiliated Hospital of Xi'an Jiaotong University, Xi'an, Shaanxi, 710061, China
Xue-Feng Yu – Materials Interfaces Center, Shenzhen Institutes of Advanced Technology, Chinese Academy of Sciences, Shenzhen 518055, P. R. China; orcid.org/0000-0003-2566-6194
Niko Hildebrandt – nanoFRET.com, Laboratoire COBRA, Université de Rouen Normandie, CNRS, INSA, 76821 Mont-Saint-Aignan, France. Department of Chemistry, Seoul National University, Seoul 08826, South Korea; orcid.org/0000-0001-8767-9623

Author Contributions

C.L. and X.W contributed equally to this work.

Author Contributions

C.L. and Z.J. designed the experiments. C.L., X.W. performed the experiments. H.Z. collected and treated real samples. C.L. wrote the manuscript. C.L., N. H., Z.J., M.Z, X.-F. Y and Q.-Y.L. analyzed the data and revised the manuscript. The manuscript was written through contributions of all authors. All authors have given approval to the final version of the manuscript.

Notes

The authors declare no competing financial interest.

ACKNOWLEDGMENT

We thank Lumiphore for the gift of Lumi4 reagents. This work was supported by the National Natural Science Foundation of China (32171392, 21805021, 21505150), the Shenzhen Sustainable Development Project (KCXFZ202002011008124), China Postdoctoral Science Foundation (2020M683449), the Natural Science Foundation of Shaanxi province (2021JQ-009), the Fundamental Research Funds for the Central Universities, and the "Young Talent Support Plan" of Xi'an Jiaotong University, China (No. YX6J001).

REFERENCES

(1) Xiong, Y.; Zhang, J. J.; Yang, Z. L.; Mou, Q. B.; Ma, Y.; Xiong, Y. H.; Lu, Y., Functional DNA Regulated CRISPR-Cas12a Sensors for Point-of-Care Diagnostics of Non-Nucleic-Acid Targets. *J. Am. Chem. Soc.* **2020,** *142* (1), 207-213.

(2) Liu, R. D.; McConnell, E. M.; Li, J. X.; Li, Y. F., Advances in functional Nucleic Acid Based Paper Sensors. *J. Mat. Chem. B* **2020,** *8* (16), 3213-3230.

(3) Liu, J. W.; Cao, Z. H.; Lu, Y., Functional Nucleic Acid Sensors. *Chem. Rev.* **2009,** *109* (5), 1948-1998.

(4) Zhang, C.-H.; Tang, Y.; Sheng, Y.-Y.; Wang, H.; Wu, Z.; Jiang, J.-H., Ultrasensitive Detection of Micrornas Using Catalytic Hairpin Assembly Coupled with Enzymatic Repairing Amplification. *Chem. Commun.* **2016,** *52* (93), 13584-13587.

(5) Song, W.; Zhang, Q.; Sun, W., Ultrasensitive Detection of Nucleic Acids by Template Enhanced Hybridization Followed by rolling Circle Amplification and Catalytic Hairpin Assembly. *Chem. Commun.* **2015,** *51* (12), 2392-2395.

(6) Zhuang, J.; Lai, W.; Chen, G.; Tang, D., A Rolling Circle Amplification-Based DNA Machine for miRNA Screening Coupling Catalytic Hairpin Assembly with DNAzyme Formation. *Chem. Commun.* **2014,** *50* (22), 2935-2938.

(7) Cai, J.; Li, X.; Yue, X.; Taylor, J. S., Nucleic Acid-Triggered Fluorescent Probe Activation by the Staudinger Reaction. *J. Am. Chem. Soc.* **2004,** *126* (50), 16324-16325.

(8) Heffern, M. C.; Matosziuk, L. M.; Meade, T. J., Lanthanide Probes for Bioresponsive Imaging. *Chem. Rev.* **2014,** *114* (8), 4496-4539.

(9) Eliseeva, S. V.; Buenzli, J.-C. G., Lanthanide Luminescence for Functional Materials and Bio-Sciences. *Chem. Soc. Rev.* **2010,** *39* (1), 189-227.

(10) Bunzli, J.-C. G., Lanthanide Light for Biology and Medical Diagnosis. *J. Lumines.* **2016,** *170*, 866-878.

(11) Cho, U.; Chen, J. K., Lanthanide-Based Optical Probes of Biological Systems. *Cell Chem. Biol.* **2020,** *27* (8), 921-936.

(12) Zhang, K. Y.; Yu, Q.; Wei, H. J.; Liu, S. J.; Zhao, Q.; Huang, W., Long-Lived Emissive Probes for Time-Resolved Photoluminescence Bioimaging and Biosensing. *Chem. Rev.* **2018,** *118* (4), 1770-1839.

(13) Sun, G.; Xie, Y.; Sun, L.; Zhang, H., Lanthanide Upconversion and Downshifting Luminescence for Biomolecules Detection. *Nanoscale Horiz.* **2021,** *6* (10), 766-780.

(14) Wang, Z.; Qiu, X.; Xi, W.; Tang, M.; Liu, J.; Jiang, H.; Sun, L., Tailored upconversion nanomaterial: A hybrid nano fluorescent sensor for evaluating efficacy of lactate dehydrogenase inhibitors as anticancer drugs. *Sens. Actuator B-Chem.* **2021,** *345*, 130417.

(15) Zhang, M.; Qu, Z.-b.; Ma, H.-Y.; Zhou, T.; Shi, G., DNA-Based Sensitization of Tb^{3+} Luminescence Regulated by Ag^{+} and Cysteine:

Use as A Logic Gate and A H_2O_2 Sensor. *Chem. Commun.* **2014,** *50* (36), 4677-4679.

(16) Zhang, M.; Le, H.-N.; Jiang, X.-Q.; Yin, B.-C.; Ye, B.-C., Time-Resolved Probes Based on Guanine/Thymine-Rich DNA-Sensitized Luminescence of Terbium(III). *Anal. Chem.* **2013,** *85* (23), 11665-11674.

(17) Balcarova, Z.; Brabec, V., Reinterpretation of Fluorescence of Terbium Ion-DNA Complexes. *Biophys. Chem.* **1989,** *33* (1), 55-61.

(18) Ci, Y. X.; Li, Y. Z.; Liu, X. J., Selective Determination of DNA by its Enhancement Effect on the Fluorescence Eu^{3+}-Tetracycline Complex. *Anal. Chem.* **1995,** *67* (11), 1785-1788.

(19) Fu, P. K. L.; Turro, C., Energy Transfer from Nucleic Acids to Tb(III): Selective Emission Enhancement by Single DNA Mismatches. *J. Am. Chem. Soc.* **1999,** *121* (1), 1-7.

(20) Alpha, B.; Ballardini, R.; Balzani, V.; Lehn, J. M.; Perathoner, S.; Sabbatini, N., Antenna Effect in Luminescent Lanthanide Cryptates - A Photophysical Study. *Photochem. Photobiol.* **1990,** *52* (2), 299-306.

(21) Prat, O.; Lopez, E.; Mathis, G., Europium(III) Cryptate - A Fluorescent Label for The Detection of DNA Hybrids on Solid Support. *Anal. Biochem.* **1991,** *195* (2), 283-289.

(22) Bazin, H.; Trinquet, E.; Mathis, G., Time Resolved Amplification of Cryptate Emission: A Versatile Technology to Trace Biomolecular Interactions. *J. Biotechnol.* **2002,** *82* (3), 233-50.

(23) Xiao, M.; Selvin, P. R., Quantum Yields of Luminescent Lanthanide Chelates and Far-Red Dyes Measured by Resonance Energy Transfer. *J. Am. Chem. Soc.* **2001,** *123* (29), 7067-7073.

(24) Brunet, E.; Juanes, O.; Sedano, R.; Rodriguez-Ubis, J. C., Lanthanide Complexes of Polycarboxylate-Bearing Dipyrazolylpyridine Ligands with Near-Unity Luminescence Quantum Yields: The Effect of Pyridine Substitution. *Photochem. Photobiol. Sci.* **2002,** *1* (8), 613-618.

(25) Bourdolle, A.; Allali, M.; Mulatier, J.-C.; Le Guennic, B.; Zwier, J. M.; Baldeck, P. L.; Buenzli, J.-C. G.; Andraud, C.; Lamarque, L.; Maury, O., Modulating the Photophysical Properties of Azamacrocyclic Europium Complexes with Charge-Transfer Antenna Chromophores. *Inorg. Chem.* **2011,** *50* (11), 4987-4999.

(26) Xu, J. C., T. M. Moore, E. G. Law, G. L. Butlin, N. G. Raymond, K. N., Octadentate CAGes of Tb(III) 2-Hydroxyisophthalamides: A New Standard for Luminescent Lanthanide Labels. *J. Am. Chem. Soc.* **2011,** *133* (49), 19900-10.

(27) Qiu, X.; Guo, J. J.; Jin, Z. W.; Petreto, A.; Medintz, I. L.; Hildebrandt, N., Multiplexed Nucleic Acid Hybridization Assays Using Single-FRET-Pair Distance-Tuning. *Small* **2017,** *13* (25).

(28) Qiu, X.; Hildebrandt, N., Rapid and Multiplexed MicroRNA Diagnostic Assay Using Quantum Dot-Based Forster Resonance Energy Transfer. *ACS Nano* **2015,** *9* (8), 8449-8457.

(29) Jin, Z. W.; Geissler, D.; Qiu, X.; Wegner, K. D.; Hildebrandt, N., A Rapid, Amplification-Free, and Sensitive Diagnostic Assay for Single-Step Multiplexed Fluorescence Detection of MicroRNA. *Angew. Chem. Int. Ed.* **2015,** *54* (34), 10024-10029.

(30) Deng, R.; Zhang, K.; Li, J., Isothermal Amplification for MicroRNA Detection: From the Test Tube to the Cell. *Acc. Chem. Res.* **2017,** *50* (4), 1059-1068.

(31) Bartel, D. P., MicroRNAs: Genomics, Biogenesis, Mechanism, and Function. *Cell* **2004,** *116* (2), 281-297.

(32) Ameres, S. L.; Horwich, M. D.; Hung, J.-H.; Xu, J.; Ghildiyal, M.; Weng, Z.; Zamore, P. D., Target RNA-Directed Trimming and Tailing of Small Silencing RNAs. *Science* **2010,** *328* (5985), 1534-1539.

(33) Ameres, S. L.; Zamore, P. D., Diversifying MicroRNA Sequence and Function. *Nat. Rev. Mol. Cell Biol.* **2013,** *14* (8), 475-488.

(34) Lujambio, A.; Lowe, S. W., The Microcosmos of Cancer. *Nature* **2012,** *482* (7385), 347-355.

(35) Mitchell, P. S.; Parkin, R. K.; Kroh, E. M.; Fritz, B. R.; Wyman, S. K.; Pogosova-Agadjanyan, E. L.; Peterson, A.; Noteboom, J.; O'Briant, K. C.; Allen, A.; Lin, D. W.; Urban, N.; Drescher, C. W.; Knudsen, B. S.; Stirewalt, D. L.; Gentleman, R.; Vessella, R. L.; Nelson, P. S.; Martin, D. B.; Tewari, M., Circulating MicroRNAs as Stable Blood-Based Markers for cancer Detection. *Proc. Natl. Acad. Sci. U. S. A.* **2008,** *105* (30), 10513-10518.

(36) Frampton, A. E.; Gall, T. M. H.; Castellano, L.; Stebbing, J.; Jiao, L. R.; Krell, J., Towards A Clinical Use of miRNAs in pancreatic cancer biopsies. *Expert Rev. Mol. Diagn.* **2013,** *13* (1), 31-34.

(37) de Planell-Saguer, M.; Celina Rodicio, M., Detection Methods for MicroRNAs in Clinic Practice. *Clin. Biochem.* **2013,** *46* (10-11), 869-878.

(38) WHO. Diagnostic Detection of 2019-nCoV by Real-Time RT-PCR. 2020.

Table of Contents